Available online at www.sciencedirect.com
SCIENCE DIRECT
Polymer 47 (2006) 849–857
polymer
www.elsevier.com/locate/polymer

The influence of incompatibility and dielectric contrast on the electric field-induced orientation of lamellar block copolymers

A. Böker [a,*], K. Schmidt [a], A. Knoll [a,1], H. Zettl [a], H. Hänsel [a], V. Urban [d,2], V. Abetz [c], G. Krausch [a,b,*]

[a] *Lehrstuhl für Physikalische Chemie II, Universität Bayreuth, Universitatsstrasse 30, D-95440 Bayreuth, Germany*
[b] *Bayreuther Zentrum für Kolloide und Grenzflächen, Universität Bayreuth, D-95440 Bayreuth, Germany*
[c] *GKSS-Forschungszentrum Geestacht GmbH, Institut für Polymerforschung, Max–Planck–Strasse, D-21502 Geesthacht, Germany*
[d] *European Synchrotron Radiation Facility (ESRF), F-38043 Grenoble, France*

Received 20 June 2005; received in revised form 17 November 2005; accepted 22 November 2005
Available online 15 December 2005

Abstract

We investigate the influence of incompatibility and dielectric contrast on the reorientation kinetics of concentrated solutions of lamellar block copolymers in the presence of an external DC electric field. We study solutions of AC diblock copolymer and ABC triblock terpolymers. The inclusion of a short, polar middle block B is used to tailor both the degree of incompatibility and the dielectric contrast between the two majority phases. In situ synchrotron radiation small-angle X-ray scattering is used to monitor the reorientation process. For the AC diblock copolymer sample only weak electric field induced reorientation could be achieved, following a very slow kinetics, whereas for the ABC triblock terpolymer, reorientation is observed above a threshold value of 0.3 kV/mm. The orientation kinetics is well described by a single exponential with characteristic time constants varying between a few seconds and several minutes depending on the polymer concentration and the electric field strength. We identify a narrow concentration window, in which the interplay between chain mobility and gain in free energy in the electric field allows the preparation of highly anisotropic bulk polymer samples by exposure to an electric field. The results are compared to free energy calculations revealing a distinct difference in the driving force for reorientation as a consequence of an increase in dielectric contrast and chain mobility upon introduction of the B middle block.

Keywords: Block copolymers; Electric field; Microdomain orientation

1. Introduction

In the recent past, the alignment of block copolymer microdomains by means of an electric field has attracted increasing interest as an alternative to mechanical fields [1–5], especially as macroscopically aligned bulk samples are of considerable technological interest [6]. So far, it has been shown that both lamellar and cylindrical microdomain structures in PS-*b*-PMMA could be oriented macroscopically in the melt using a DC electric field [7–12]. Due to the dielectric contrast $\Delta\varepsilon$ between the blocks ($\varepsilon_{PS} \approx 2.4$, $\varepsilon_{PMMA} \approx 3.6$) [13], the microdomains tend to orient parallel to the electric field vector thereby lowering the free energy of the system. Because of the high melt viscosities, temperatures close to the decomposition temperature and electric field strengths up to 25 kV/mm are required to achieve high degrees of orientation. In recent studies [14–16], we have demonstrated that electric field induced alignment can be applied successfully to block copolymer solutions at room temperature and at electric field strengths around 1 kV/mm as well, thereby effectively circumventing limitations associated with the high melt viscosities of high molecular weight copolymers or copolymers of more complex architectures (multiblock copolymers, star copolymers, etc). In our previous investigations on solvent-based systems, the interplay between (i) viscosity (i.e. chain mobility) and (ii) dielectric contrast (i.e. electric driving force) turned out to be critical.

In the present study we modify the effective dielectric contrast and the degree of incompatibility between the blocks

* Corresponding authors. Tel.: +49 921 552 335; fax: +49 921 552 059.
E-mail addresses: alexander.boeker@uni-bayreuth.de (A. Böker), georg.krausch@uni-bayreuth.de (G. Krausch).
[1] Present address. IBM Research GmbH, Zurich Research Laboratory, CH-8803 Rüschlikon, Switzerland.
[2] Present address. Oak Ridge National Laboratory (ORNL), Oak Ridge, TN 37831, USA.

0032-3861/$ - see front matter © 2005 Elsevier Ltd. All rights reserved.
doi:10.1016/j.polymer.2005.11.069

of a lamellar polystyrene-*b*-poly(methyl methacrylate) AC diblock copolymer by inclusion of a short, polar poly(2-hydroxyethyl methacrylate) middle block, which mixes with the poly(methyl methacrylate) end block [14]. We explore the kinetics and mechanisms of the microdomain reorientation using real-time synchrotron small angle X-ray scattering (SAXS) measurements. With ex situ SAXS we show that—in contrast to the AC diblock—the ABC triblock yields highly aligned bulk samples after solvent casting under an applied electric field. Finally, we compare the experimental observations with free energy calculations, revealing a distinct difference in the driving force for reorientation accompanied by a decrease in viscosity for the phase separated system (induced by a decrease of the order–disorder concentration in solution) as a consequence of an increase in dielectric contrast upon introduction of poly(2-hydroxyethyl methacrylate) into the methacrylic phase.

2. Experimental section

2.1. Synthesis

The polystyrene-*b*-poly(2-hydroxyethyl methacrylate)-*b*-poly(methyl methacrylate) triblock terpolymer was synthesized by sequential living anionic polymerization as described in detail elsewhere [17]. The polymer used in this study consists of 47 wt% polystyrene (PS), 10 wt% poly(2-hydroxyethyl methacrylate) (PHEMA) and 43 wt% poly (methyl methacrylate) (PMMA) with a total number-average molecular weight $M_n = 82{,}000$ g/mol (we denote this material as $S_{47}H_{10}M_{43}^{82}$). GPC of the final block copolymer yields a polydispersity of $M_w/M_n = 1.04$. The block ratio and overall molecular weight were determined by ^{1}H NMR using the integrated aromatic signals of the polystyrene block of the final polymer in combination with the GPC results of the corresponding polystyrene precursor. The polystyrene-*b*-poly(methyl methacrylate) diblock copolymer was synthesized and characterized analogously, yielding $M_n = 100{,}000$ g/mol and $M_w/M_n = 1.03$ with nearly symmetrical composition (49 wt% PS, 51 wt% PMMA, denoted as $S_{49}M_{51}^{100}$).

2.2. Sample preparation

Block copolymer solutions in THF with polymer concentrations between 30 and 70 wt% were used for the present study. The alignment experiments were performed in a home-built closed capacitor with gold electrodes (sample depth = 5 mm, electrode distance $d = 1$–2 mm; Fig. 1) at 25 °C. A DC voltage between 0.25 and 3 kV/mm was applied across the electrodes resulting in an electric field perpendicular to the X-ray beam direction. Both the voltage at the electrodes and the current were monitored during the course of the experiment indicating only a small leakage current within the sensitivity of the setup ($I \approx 0.01$ mA) during the first few seconds after the field was applied. During this period, no lamellar reorientation was detected.

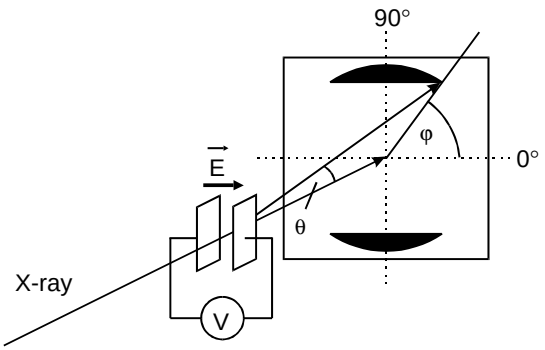

Fig. 1. Sketch of the experimental setup for in situ synchrotron small angle X-ray scattering (SAXS) experiments at the ID2 beamline at the European Synchrotron Radiation Facility (ESRF) in Grenoble, France.

Oriented melt samples were produced via solvent casting from chloroform using an open cylindrical capacitor with aluminum electrodes ($r = 5$ mm, $d = 1.1$ mm) at 25 °C. Due to its low flammability we used chloroform for safety reasons; for SAXS, however, THF had to be employed because of the low X-ray transmission of $CHCl_3$. The details of this setup have already been described elsewhere [14].

2.3. Synchrotron small-angle X-ray scattering (synchrotron-SAXS)

Synchrotron-SAXS measurements were performed at the ID2 beamline at the European Synchrotron Radiation Facility (ESRF, Grenoble, France). The typical photon flux routinely obtained at the ID2 sample position is 10^{13} photons/s at an energy width $\Delta E/E = 2 \times 10^{-4}$. The operating beam energy was 12.5 keV, corresponding to a peak wavelength of 0.1 nm. The beam direction (cross section: 200×200 μm^2) was perpendicular to the direction of the applied electric field.

The detector system is housed in a 10 m evacuated flight tube. An image intensified CCD detector was used, which can handle the full X-ray flux. The CCD detector is capable of acquiring up to 10 frames of 1024×1024 pixels per second and a sequence of up to 125 frames can be acquired with this time resolution. Prior to data analysis, background scattering was subtracted from the data and corrections were made for spatial distortions and for the detector efficiency.

2.4. Calculation of order parameters

As will become clear from the experimental observations described below, domain alignment is influenced by two competing external fields of different symmetry, i.e. the interfacial field between polymer solution and the electrode surfaces and the electric field, respectively. To quantify the microdomain alignment, we calculate the order parameter P_2 by integrating the scattering intensity $I_q(\varphi)$ over the azimuthal angle φ from $\varphi = 0$–360°:

$$P_2 = \frac{3\langle \cos^2 \varphi \rangle - 1}{2} \quad (1)$$

with

$$\langle \cos^2\varphi \rangle = \frac{\int_0^{2\pi} \mathrm{d}\varphi (I_q(\varphi)\cos^2(\varphi)|\sin(\varphi)|)}{\int_0^{2\pi} \mathrm{d}\varphi (I_q(\varphi)|\sin(\varphi)|)} \quad (2)$$

Depending on the type of alignment, two different ranges of the order parameter exist. For lamellar alignment parallel to the electrodes (maximum scattering intensity at $\varphi = 0°$), P_2 ranges from 0 to 1 with $P_2 = 1$ corresponding to perfect lamellar alignment parallel to the electrodes. For an alignment of the lamellae along the field direction (maximum scattering intensity at $\varphi = 90°$), P_2 ranges from 0 to -0.5 with $P_2 = -0.5$ corresponding to the perfectly oriented case. We note, however, that 'perfect orientation' still allows for an isotropic distribution of the lamellae's normals within the plane perpendicular to the electric field direction.

In order to quantify the orientation kinetics, the orientational order parameter P_2 was calculated for each single scattering pattern acquired during the course of the experiment. The behavior of P_2 as a function of time t has been fitted by a single exponential as described by:

$$P_2(t) = P_{2,\infty} + (P_{2,0} - P_{2,\infty})\mathrm{e}^{-t/\tau} \quad (3)$$

with $P_{2,0}$ and $P_{2,\infty}$ being the limiting values of the order parameter before application of the electric field and at late times, respectively, and τ being the time constant.

The remainder of the paper is organized as follows. We shall first investigate the structure formation of $S_{47}H_{10}M_{43}^{82}$ in solution in the absence of the electric field. We then continue discussing the influence of an external electric field on the domain orientation of solutions of different concentrations and at different electric field strengths. Finally, we compare the observed kinetic behavior of the $S_{47}H_{10}M_{43}^{82}$ with $S_{49}M_{51}^{100}$ block copolymers and discuss the results in view of free energy calculations.

3. Results and discussion

3.1. Structure formation in the absence of an electric field

An external electric field can only align a microphase-separated structure. Therefore, we studied the microdomain structure of the $S_{49}M_{51}^{100}$ diblock and $S_{47}H_{10}M_{43}^{82}$ triblock copolymer in THF solution with SAXS as a function of polymer concentration, starting from $w_p = 30$ wt% and increasing w_p stepwise by 2.5 wt% up to 60 wt% in order to determine the order–disorder concentration w_{ODT} of the block copolymer systems. From these measurements we find that for the $S_{49}M_{51}^{100}$ diblock copolymer the w_{ODT} is localized around 53 wt% (not shown here).

For the $S_{47}H_{10}M_{43}^{82}$ triblock copolymer, we find the formation of a narrow first-order Bragg reflection when increasing the concentration from 37.5 to 40 wt% (Fig. 2). We note that starting from 40 wt% the block copolymer solution becomes birefringent. At higher concentrations we observe a third order scattering peak, indicating the formation of lamellar microdomains in the solution. The fact that the second order peak is suppressed in the SAXS patterns can be attributed to a minimum in the structure factor, which would be expected for a binary lamellar structure with equal lamellar thickness. As indicated above, we expect the PHEMA and PMMA to form a mixed phase. In consequence, the scattering experiment effectively probes a binary lamellar structure consisting of successive layers of PHEMA/PMMA and PS, respectively. This structure exhibits mirror symmetry at the centre of any microphase, resulting in the observed suppression of even harmonics in the scattering pattern.

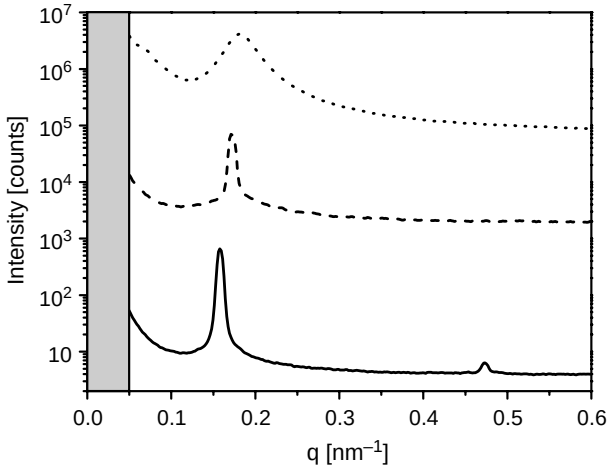

Fig. 2. Scattering intensity profiles of $S_{47}H_{10}M_{43}^{82}$ solutions in THF at various concentrations. 37.5 wt% (···), 40 wt% (– – –), 47.5 wt% (—).

From the above described findings, we locate the order–disorder transition (ODT) for the $S_{47}H_{10}M_{43}^{82}$ triblock copolymer at room temperature at around $w_{ODT} \approx 40$ wt%. Obviously, the presence of the PHEMA middle block leads to an increased incompatibility and thereby to a lower order–disorder concentration. Thus, the viscosity of solutions just above the order–disorder concentration w_{ODT} is significantly lowered by the inclusion of the PHEMA middle block.

3.2. Reorientation behavior

After sample preparation and prior to electric field exposure, all phase-separated solutions exhibit a distinctly anisotropic scattering pattern with maxima located at $\varphi = 0$ and 180° (Fig. 3(A)). This pattern indicates alignment of the lamellae parallel to the electrodes. Such an alignment can be caused both by preferential interaction of PS with the gold surfaces and by shear forces acting on the highly viscous solutions during the filling of the capacitor with a syringe [18].

The lowest possible concentration (and thus viscosity) to give a phase separated polymer solution for the $S_{49}M_{51}^{100}$ diblock copolymer system was found at 53 wt% in THF. Here, only slow reorientation of the microdomains could be realized at a field strength of 2 kV/mm as shown in Fig. 4(B). We note that the data shown here represent the fastest possible realignment kinetics achievable for the $S_{49}M_{51}^{100}$ system, as with increasing polymer concentration, the viscosity immediately dominates

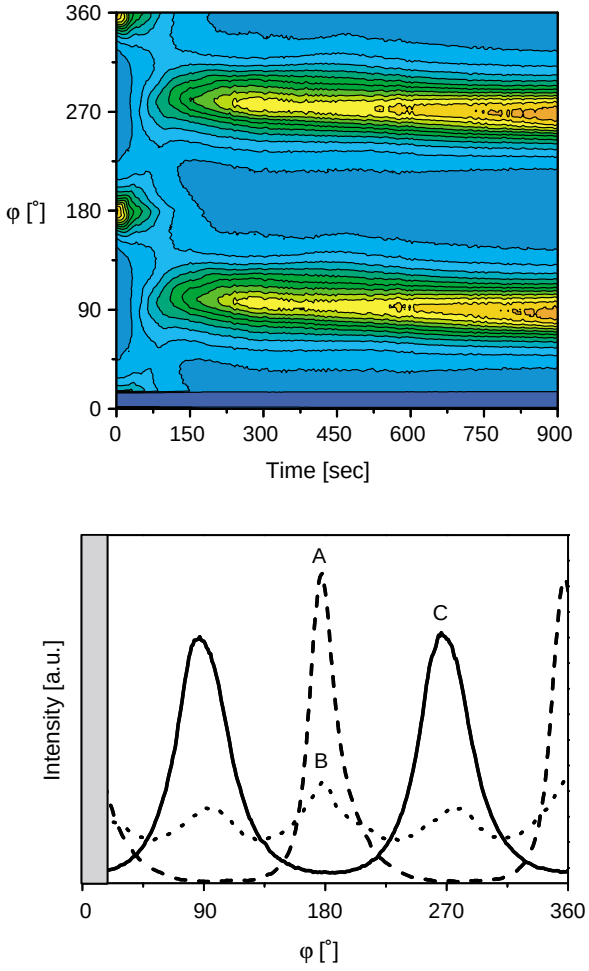

Fig. 3. (top) Time development of the azimuthal angular dependence of the scattering intensity of a 40 wt% solution of $S_{47}H_{10}M_{43}^{82}$ in THF at 1 kV/mm (electrode spacing, 1 mm). (bottom) Azimuthal scattering intensity at (A) $t=0$ s, (B) $t=100$ s, (C) $t=900$ s.

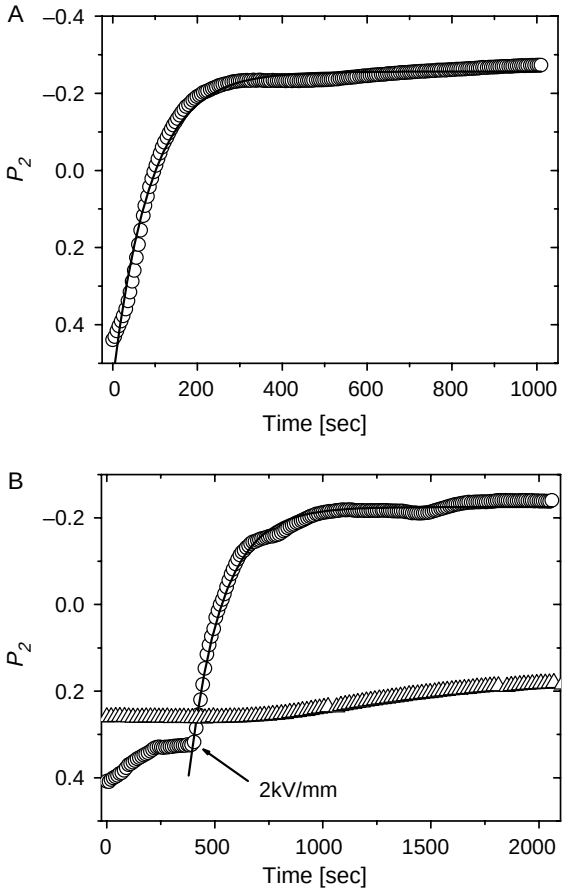

Fig. 4. Evolution of orientational order parameter P_2 with time (for orientation parallel to the electric field vector): (A) 40 wt% solution of $S_{47}H_{10}M_{43}^{82}$ in THF at 1 kV/mm; (B) 45 wt% solution of $S_{47}H_{10}M_{43}^{82}$ in THF at 1 kV/mm and 2 kV/mm (○). For comparison, the data for a 53 wt% solution of $S_{49}M_{51}^{100}$ in THF at 1 and 2 kV/mm is added (△). The solid lines represent least squares fits to the data. Electrode spacing, 1 mm.

the process, rendering the reorientation impossible. Obviously, above w_{ODT} the force implied on the lamellae is not sufficient to lead to significant reorientation [14], rearranging the microstructure in a highly viscous solution.

In the triblock copolymer case a different behavior is observed. As soon as an electric field of 1 kV/mm is applied to a 40 wt% solution, the scattering pattern changes significantly. The peaks at $\varphi=0$ and 180° decrease and new scattering maxima at $\varphi=90$ and 270° grow with time (Fig. 3(A)–(C)).

3.3. Concentration dependence

The kinetics of the microdomain alignment was followed within a narrow concentration window between the order–disorder concentration $w_{ODT}\approx 40$ and 50 wt% for the SHM polymer. As can be seen from Fig. 4 and Table 1, the time constants for the reorientation process at 1 kV/mm are in the range of some minutes (1.5 min for 40 wt% and almost 6 min for 45 wt%, respectively). At concentrations above 45 wt% no electric field induced orientation could be detected. Moreover, at 45 wt% (Fig. 4(B)) the process is slowed down significantly at an incomplete degree of alignment ($P_2=0.28$), which can only be overcome by increasing the field strength. At a polymer concentration of 50 wt%, within the experimental time window of several minutes no microdomain orientation could be achieved at field strengths as high as 6 kV/mm. The results of the exponential fits are summarized in Table 1. The single exponential fit works quite well for all concentrations studied, as can be seen from the low χ^2 values. At a sufficiently high electric field strength, P_2 reaches about the same limiting values $P_{2,\infty}=-0.25\pm0.02$ independent of concentration.

We note that the behavior displayed in Fig. 4 results from a delicate balance between an increase of both the driving force

Table 1
Time constants τ of the reorientation behavior of $S_{47}H_{10}M_{43}^{82}$ at different polymer concentrations and different electric field strengths E obtained from least squares fits using Eq. (3) (1 mm electrode spacing)

Concentration (wt%)	E (kV/mm)	τ (s)	$P_{2,\infty}$	χ^2 (10^{-4})
40	1	89	−0.26	3.8
45	1	348	0.28	0.5
45	2	157	−0.23	1.4
45	3	151	−0.27	0.6

for reorientation (i.e. a larger dielectric contrast) and the viscous retardation as the polymer concentration is increased [15]. The exact behavior is difficult to predict; however, the data shown in Fig. 4 and Table 1 indicate that in the particular system studied here the increase in viscosity dominates over the increase of the driving force. Therefore, the reorientation process slows down with increasing polymer concentration. For a sufficiently high electric field strength the viscosity only influences the kinetics but not the final degree of order ($P_{2,\infty}$), which is consistent with previous dielectric relaxation spectroscopy measurements on the realignment of a side-chain liquid crystalline polymer in its liquid-crystalline state induced by a DC electric field [19].

If this procedure was to be used for the preparation of macroscopically aligned bulk samples, the alignment process should be faster than the time needed for solvent evaporation. From the above results we conclude that concentrations between 40 and 45 wt% are suitable for the preparation of dried bulk samples by solvent casting. Fig. 5 shows the feasibility of such a process. Using a home-built capacitor which allows application of an electric DC field during film formation by solvent casting [14], a melt sample of 1 mm thickness dried in the presence of an electric field of 2 kV/mm was prepared from a 25 wt% solution in chloroform (comparable to 40 wt% in THF). After complete drying of the solution, the resulting film was cut to a 1 mm^3 cubicle and a SAXS patterns was monitored with the X-ray beam perpendicular to the electric field vector. From the azimuthal angular dependence of the scattering intensity at the first order reflexion, we calculate $P_2 = -0.4$. Here we note that the similar process with the $S_{49}M_{51}^{100}$ diblock copolymer system did not yield anisotropic bulk samples.

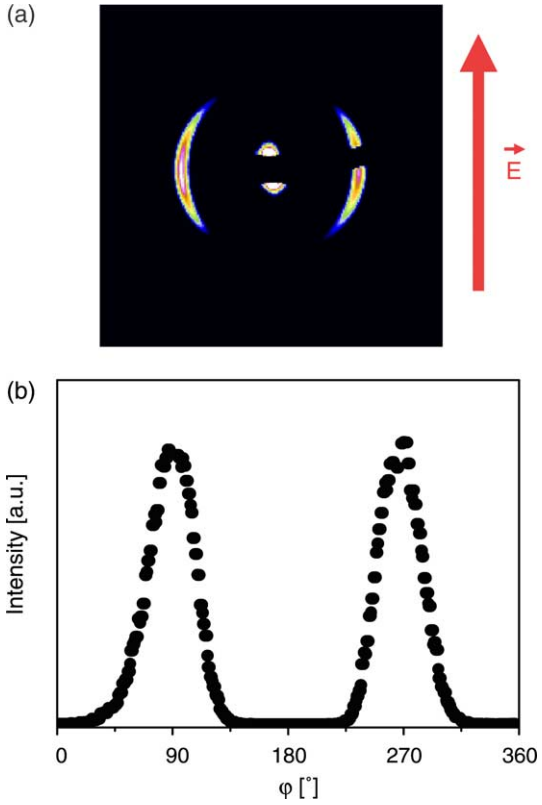

Fig. 5. SAXS data of a $S_{47}H_{10}M_{43}^{82}$ bulk sample prepared from a 25 wt% solution in chloroform dried under an applied electric field of 2 kV/mm (electrode spacing, 1 mm). (A) 2D-SAXS pattern and (B) azimuthal intensity distribution at first-order reflection ($P_2 = -0.4$) [14].

3.4. Electric field strength dependence

In another set of experiments, we varied the electric field strength between 0.25 and 3 kV/mm to probe its influence on the reorientation kinetics. In this case a 40 wt% solution of SHM in THF was studied at room temperature. A selection of P_2 versus t curves is shown in Fig. 6. The results of the fitting procedure are summarized in Table 2 and displayed in Fig. 7. The quality of the single exponential fits can again be inferred from the low χ^2 values. Except for $E = 0.375$ kV/mm ($P_{2,\infty} = -0.08$), the limiting values of the order parameter, $P_{2,\infty}$, always reach a value around $P_{2,\infty} = -0.2 \pm 0.03$. With increasing field strength, there is a slight tendency towards higher plateau values (-0.17 to -0.22). The time constants, τ range from 545 s for low electric fields (0.375 kV/mm) to as low as 0.64 s for the highest field strength (3 kV/mm). We were not able to detect any reorientation for electric fields at and below 0.25 kV/mm. We may, therefore, conclude that there exists a threshold field strength $E_t = 0.25$–0.375 kV/mm, below which no field induced reorientation is possible. One has to realize, though, that whether or not a field induced reorientation is observed may well depend on the time scale of the experiment. Indeed, if we monitor the reorientation kinetics in detail (as shown in Fig. 6), we find that the process is slowed down significantly if the electric field strength is decreased. In consequence, the time needed to achieve any measurable change in the scattering pattern will increase with decreasing field strength as well. Therefore, both in the melt experiments as well as in the experiments reported here, the exact value of the threshold electric field to some extent will

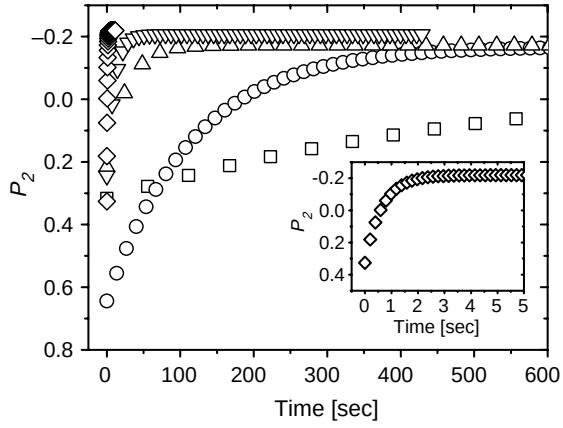

Fig. 6. Evolution of orientational order parameter P_2 with time for 40 wt% solutions at different field strengths (□ = 375 V/mm, $\tau = 545$ s; ○ = 500 V/mm, $\tau = 116$ s; △ = 1 kV/mm, $\tau = 18.7$ s; ▽ = 1.5 kV/mm, $\tau = 10.3$ s; ◇ = 3 kV/mm, $\tau = 0.64$ s). Electrode spacing, 2 mm.

Table 2
Time constants τ of the reorientation behavior of $S_{47}H_{10}M_{43}^{82}$ at different field strength E obtained from least squares fits using Eq. (3) (w_p=40 wt%, 2 mm electrode spacing)

E (kV/mm)	τ (s)	$P_{2,\infty}$	χ^2 (10^{-5})
0.25	[a]	[a]	[a]
0.375	545	−0.08	5.0
0.5	116.2	−0.17	4.1
0.75	32	−0.16	5.5
1	18.7	−0.17	4.8
1.25	12.7	−0.20	2.5
1.5	10.3	−0.21	2.6
1.75	5.6	−0.21	3.2
2	2.9	−0.20	4.8
2.25	2	−0.21	3.9
2.5	1.3	−0.21	3.1
3	0.64	−0.22	2.9

[a] No electric field induced reorientation observed.

depend on the time allowed for reorientation. From our kinetic experiments we can define the threshold electric field strength as the value of the electric field at which the time constant for reorientation diverges. Above E_t, the time constant scales with the electric field strength described by a hyperbolic power law $\tau=\alpha(E-E_t)^a+\tau_\infty$. The data points are best fitted for α= 0.10 s, $a=-1.47$, E_t=310 V/mm and τ_∞=0 s (solid line in Fig. 7). The asymptotic behavior at high electric field strength (i.e. for a large force acting on the lamellae), yielding τ_∞=0 s for infinite field strength is expected in the absence of any electrorheological effects and limits in single chain diffusion, as the dominating process at w_p=40 wt% is the migration of grain boundaries. The asymptotic behavior at low field indicates a threshold field strength, E_t=310 V/mm.

This threshold value can be explained by a competition between the electric field and the surface field generated by the gold electrodes. The latter exhibits a rather wide range, as has already been found by Anastasiadis et al. for PS-*b*-PMMA block copolymer films without an external field [18]. In a recent theoretical work, Tsori and Andelman [20] have described the different threshold fields expected for a strongly phase separated system. We typically find some 10 lamellar layers oriented parallel to the polymer–electrode interface with a transition to lamellae perpendicular to the electrodes [14]. We, therefore, conclude that our system exhibits a mixed orientation as considered by Tsori and Andelman. In this state, the system has to compensate a positive energy penalty associated with the formation of T-junctions for the transition from lamellae parallel to perpendicular to the boundary surfaces, which mainly depends on the dielectric contrast of the block copolymer system and the sample thickness. This penalty has to be balanced by the electric field. Therefore, we can define the threshold field strength as the voltage needed to overcome this energetic barrier.

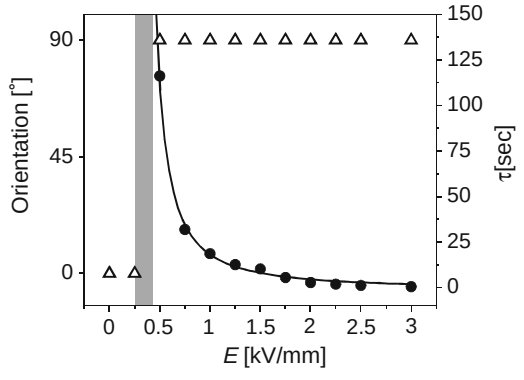

Fig. 7. The achieved orientation at the respective field strength is represented by open triangles (0°, alignment parallel to the electrodes; 90°, alignment parallel to the electric field vector). The filled circles show the electric field dependence of the time constant, τ, for 40 wt% solutions at 2 mm electrode spacing. The solid line represents a least-squares fit of the power law $\tau=\alpha(E-E_t)^a+\tau_\infty$ to the data points yielding α=0.10 s, $a=-1.47$, E_t=310 V/mm and τ_∞=0 s.

3.5. Mechanism of domain alignment

Synchrotron-SAXS is an excellent tool to microscopically investigate the reorientation process as it combines the advantages of birefringence (high time resolution) with the detailed and straightforward information about the microscopic order characteristic of scattering methods.

The change in the azimuthal angular dependence of the scattering pattern as shown in Fig. 3(A)–(C), i.e. increase of scattering signals parallel to the electric field vector (φ=90°/270°) and simultaneous decrease of the peaks parallel to the electrodes (φ=0°/180°) reveals the prevailing mechanism characteristic for all processes described here. Recent dynamic density functional theory simulations by Zvelindovsky and Sevink have provided evidence that the reorientation is mainly governed by migration of grain boundaries, i.e. nucleation and growth of domains [16,21]. Immediately after the application of the electric field, the lamellae become unstable and exhibit undulations, and eventually form point like defects. These defects serve as nucleation centers for grains with lamellar orientation parallel to the electric field. As the process evolves, new instabilities are formed around the new structure contributing to the growth of the grain with lamellar orientation parallel to the electric field at the expense of the initial orientations. Furthermore, from TEM images of dried bulk samples, we have identified the typical point- or micellar-like lamellar defects as predicted by the above described simulations [15,22]. The occurrence of these isotropically oriented defects at the onset of the reorientation process may also explain the increase in isotropic scattering intensity as shown in Fig. 3(B).

3.6. Comparison of the diblock ($S_{49}M_{51}^{100}$) and the triblock ($S_{47}H_{10}M_{43}^{82}$) system

In the following we will consider electrostatic and thermodynamic arguments to discuss the different behavior observed for the PS-*b*-PMMA and the PS-*b*-PHEMA-*b*-PMMA diblock and triblock copolymers, respectively.

We aim to estimate the electrostatic energy difference between the different microdomain orientations. As indicated

by differential scanning calorimetry (DSC), rheological and TEM experiments reported earlier [14], we anticipate that PHEMA and PMMA form a mixed phase. Thus, we will treat the $S_{47}H_{10}M_{43}^{82}$ copolymer as an AB diblock copolymer with the following composition: A, 47 wt% PS ($\varepsilon_A = 2.4$) and B, 53 wt% methacrylic blocks ($\varepsilon_B = 0.81\varepsilon_{PMMA} + 0.19\varepsilon_{PHEMA} = 4.6$; with $\varepsilon_{PMMA} = 3.6$ and $\varepsilon_{PHEMA} = 8.9$). The resulting dielectric contrast amounts to $\Delta\varepsilon = 2.2$. The $S_{49}M_{51}^{100}$ diblock copolymer on the other hand is calculated with 49 wt% PS ($\varepsilon_A = 2.4$) and 51 wt% PMMA ($\varepsilon_{PMMA} = 3.6$) leading to a dielectric contrast of only $\Delta\varepsilon = 1.2$.

In order to estimate the driving forces for domain alignment as a function of the volume fraction of solvent, ϕ_s, we calculate the electric energy per unit area, W, which is stored in a capacitor for an open setup which allows for solvent evaporation (including a layer of air in the system) and a closed system as used for the in situ SAXS studies. The details of the model calculation are given elsewhere [14]. In order to keep consistency with a previous paper and allow for a straightforward comparison between open and closed system, we used chloroform for both calculations [14]. As THF and chloroform are fairly non-selective solvents for the two main components, PS and PMMA, we may assume a similar swelling behavior leading merely to a dilution effect with respect to the dielectric constants of each block. Similar calculations using THF as solvent confirmed a qualitative agreement with the results obtained for the chloroform case. With increasing solvent content the difference of the dielectric constants is reduced to $\Delta\varepsilon_{eff} = \phi_p\Delta\varepsilon$ and the thermodynamic driving force for an alignment of the lamellae parallel to the field is expected to decrease accordingly.

Film formation in the open capacitor under the influence of an external electric field may result in significant thickness undulations which eventually lead to the formation of column-like protrusions that connect both electrodes. Recently, Schäffer et al. showed that electric fields can induce electrohydrodynamic instabilities in a liquid polymer film leading to the formation of polymer columns quite similar to the ones observed here [23,24]. In between the columns, we find areas with film thicknesses ranging between 0.2 and 0.7 mm. All these parts show a significant alignment of the lamellae parallel to the electric field. The most pronounced anisotropy, however, is found within the columnar protrusions [14].

Therefore, we have chosen four basic geometries to describe the open system, corresponding to a perpendicular ($W_{\perp,col}$, $W_{\perp,flat}$) and parallel ($W_{\parallel,col}$, $W_{\parallel,flat}$) alignment of the microdomains with respect to the electric field and to a formation of columns ($W_{\perp,col}$, $W_{\parallel,col}$) and a flat film ($W_{\perp,flat}$, $W_{\perp,flat}$) in the open capacitor, respectively (Fig. 8(A)). In the case of the closed capacitor, the two perpendicular ($W_{\perp,col}$, $W_{\perp,flat} = W_\perp$) and two parallel ($W_{\parallel,col}$, $W_{\parallel,flat} = W_\parallel$) cases are equivalent.

We calculate the energy per area, W, stored within the electric field of the capacitor as

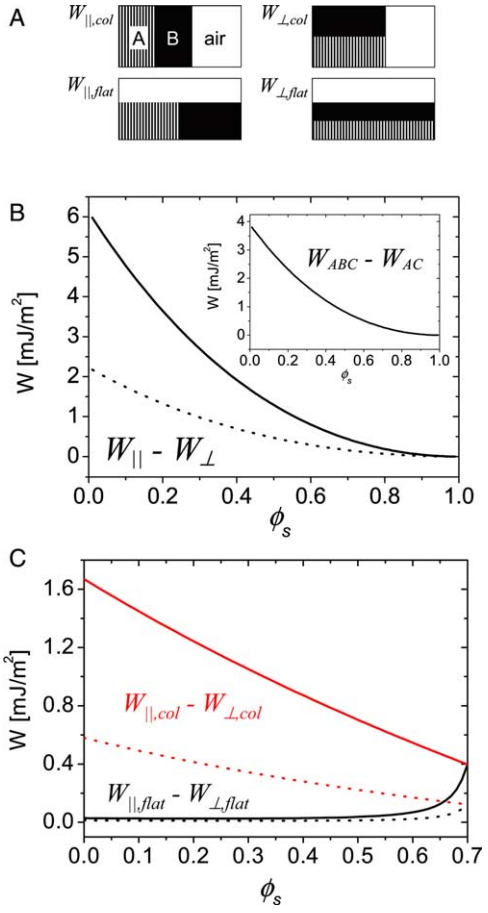

Fig. 8. (A) Four basic geometries of lamellar orientation in an open capacitor. (B) Difference in calculated energy between the orientations parallel and perpendicular to the electric field vector within a closed capacitor filled with $S_{47}H_{10}M_{43}^{82}$ (—) and $S_{49}M_{51}^{100}$ (···) solution in chloroform as a function of solvent volume fraction. The inset depicts the overall energy difference between the two polymer systems. (C) Open capacitor which allows for solvent evaporation with $S_{47}H_{10}M_{43}^{82}$ (—) and with $S_{49}M_{51}^{100}$ block copolymer (···) in $CHCl_3$, corresponding to the geometries as depicted in (A). In all calculations the field strength is 2 kV/mm.

$$\frac{W}{A} = \frac{1}{2}\int \vec{E}\cdot\vec{D}\,\frac{dV}{A} \tag{4}$$

with $\vec{E}$ being the electric field and $\vec{D}$ the displacement field.

In contrast to the dielectric displacement, $\vec{D}$, the electric field, $\vec{E}$, along the z-direction of the capacitor is not uniform for the models involving a layered structure ($W_{\perp,flat}$ and $W_{\perp,col}$). This is due to the fact that the component of the electric field perpendicular to the interface between two materials is not continuous, but the one of the displacement field is: $\vec{D}_{\perp 1} = \vec{D}_{\perp 2}$ but $\vec{E}_{\perp 1} \neq \vec{E}_{\perp 2}$. Additionally, $\vec{E}_i = \vec{D}_i/\varepsilon_i$ and the applied voltage $V = \int \vec{E}dz$, which means that as soon as air is present as a layer in the capacitor with the applied voltage V, the electric field in both polymer layers is reduced.

Fig. 8(B) shows the difference in energy between the orientations parallel and perpendicular to the electric field vector within a closed capacitor filled with different solutions of our model AB block copolymers in chloroform with $\varepsilon_A = 2.4$ and $\varepsilon_B = 4.6$ (resembling $S_{47}H_{10}M_{43}^{82}$, full line) and with $\varepsilon_A = 2.4$ and $\varepsilon_B = 3.6$ (resembling $S_{49}M_{51}^{100}$, dotted line) as

a function of solvent volume fraction ($\varepsilon_{CHCL_3} = 4.8$) at a field strength of 2 kV/mm. Compared to an open capacitor the system stores at least two times more energy at any given solvent concentration up to 60 vol% [14]. The inset depicts the overall energy difference between the above described cases, i.e. the aligned triblock terpolymer lamellae always allow the capacitor to store more energy than the diblock system.

Fig. 8(C) shows the difference in energy stored per unit area within an open capacitor filled with 15 vol% polymer A ($\varepsilon_A = 2.4$) and 15 vol% polymer B ($\varepsilon_B = 4.6$ with PHEMA and $\varepsilon_B = 3.6$ without PHEMA) as a function of $CHCl_3$ volume fraction ($\varepsilon_{CHCl_3} = 4.8$), corresponding to the four basic geometries, at a field strength of 2 kV/mm. Curves $W_{\perp,col}$ and $W_{\perp,flat}$ as well as curves $W_{\parallel,col}$ and $W_{\parallel,flat}$ converge at a solvent volume fraction of 70 vol% (which is the starting concentration of our solvent casting experiment), because at this point the capacitor is completely filled and the respective geometries are equivalent. Besides the fact that for the SHM as well as the SM system the difference in energy between the two orientations in columns ($W_{\perp,col}$, $W_{\parallel,col}$) is larger than for flat films ($W_{\perp,flat}$, $W_{\parallel,flat}$), the overall energetic difference is more than three times higher for the SHM than for the SM system.

When we compare the two situations described above, we find that: (i) the closed system stores more energy per unit area [14], (ii) the difference in energy between the two orientations ($W_{\parallel} - W_{\perp}$) is always higher for the experimentally relevant concentrations in the closed capacitor, and (iii) in all cases, the SHM system is clearly electrostatically favored as it allows the capacitor to store more energy per unit area. Therefore, from our experimental findings, we may conclude that, if the electric field induced orientation of a block copolymer does not work in the closed capacitor, it will neither function in the open system, as the energetic difference is always larger for the closed capacitor setup. Furthermore, the incorporation of the high dielectric constant PHEMA middle block into the PS-*b*-PMMA diblock copolymer is the key to increasing the electrostatic driving force of the alignment process in order to create a well-performing methacrylate-based block copolymer system for electric field induced alignment from solution.

Moreover, the PHEMA block enhances the microphase-separation in the block copolymer solutions compared to the PS-*b*-PMMA system which only phase-separates at a polymer concentration above 53 wt%, while the PHEMA containing block copolymer already microphase-separates at $w_p \geq 40$ wt%. Therefore, in the latter case, the viscosity of the phase-separated solution is considerably smaller, which promotes the ordering process induced by the small electric force. On the other hand, a lower polymer concentration also reduces the effective field strength and driving force in the capacitor as shown in Fig. 8(B) and (C).

To this point, we cannot decide definitely, if in this particular system enhanced phase separation or the increased dielectric contrast between the blocks is more important for the electric field-induced ordering process to function. So far, our results point to a delicate balance between both parameters.

4. Conclusion

Using synchrotron-SAXS we have identified nucleation and growth of domains by migration of grain boundaries as the governing mechanism of the electric field induced microdomain alignment of a PS-*b*-PHEMA-*b*-PMMA triblock terpolymer in solution. In addition, the time-resolved SAXS measurements allowed us to study the kinetic behavior of the PS-*b*-PHEMA-*b*-PMMA system compared to the PS-*b*-PMMA diblock copolymer. The interplay of enhanced microphase separation and contribution to a high dielectric contrast between the phases by incorporation of the PHEMA block results in a functioning electric field driven ordering process. Furthermore, we have identified a rather small concentration window between 40 and 45 wt% in which microdomain ordering by electric fields can be effectively realized. The variation of the electric field strength revealed a threshold value, below which no electric field induced orientation can be achieved. In summary, the maximum final orientation reached in solution could be described by order parameters of down to $P_2 = -0.27$ (the theoretical minimum value of $P_2 = -0.5$ corresponds to the maximum in orientation). The time constants of the fastest processes were in the range of $\tau = 0.6$ s. Finally, after complete solvent evaporation, bulk samples exhibited order parameters of down to $P_2 = -0.4$.

We have demonstrated that electric field alignment of block copolymer domains from solution provides a useful tool to generate anisotropic bulk block copolymer samples by controlling a large variety of parameters like block copolymer composition, polymer concentration, and electric field strength.

The application of a solvent-based procedure to the alignment of methacrylate containing block copolymers combines the high technological potential of these materials with access to an extended range of functionality and molecular weight of the respective materials.

Acknowledgements

The authors thank H. Krejtschi and his team for the skillful assistance building the capacitors, and H. Elbs for many stimulating discussions. We are grateful to the ESRF for financial support and provision of synchrotron beam time. This work was carried out in the framework of the Sonderforschungsbereich 481 (TP A2) funded by the German Science Foundation (DFG).

References

[1] Wiesner U. Macromol Chem Phys 1997;198:3319.
[2] Chen Z-R, Kornfield JA, Smith SD, Grothaus JT, Satkowski MM. Science 1997;277:1248.
[3] Chen Z-R, Kornfield JA. Polymer 1998;39:4679.
[4] Keller A, Pedemonte E, Willmouth FM. Nature 1970;225:538.
[5] Albalak RJ, Thomas EL. J Polym Sci, Polym Phys Ed 1993;31:37.
[6] Thurn-Albrecht T, Schotter J, Kastle GA, Emley N, Shibauchi T, Krusin-Elbaum L, et al. Science 2000;290:2126.

[7] Amundson K, Helfand E, Davis DD, Quan X, Patel SS, Smith SD. Macromolecules 1991;24:6546.
[8] Amundson K, Helfand E, Quan X, Smith SD. Macromolecules 1993;26: 2698.
[9] Morkved TL, Lu M, Urbas AM, Ehrichs EE, Jaeger HM, Mansky P, et al. Science 1996;273:931.
[10] Morkved TL, Lopez VA, Hahm J, Sibener SJ, Jaeger HM. Polymer 1998; 39:3871.
[11] Mansky P, DeRouchey J, Russell TP, Mays J, Pitsikalis M, Morkved TL, et al. Macromolecules 1998;31:4399.
[12] Thurn-Albrecht T, DeRouchey J, Russell TP, Jaeger HM. Macromolecules 2000;33:3250.
[13] Brandrup J, Immergut EH. Polymer handbook. 3rd ed. New York: Wiley; 1991.
[14] Böker A, Knoll A, Elbs H, Abetz V, Müller AHE, Krausch G. Macromolecules 2002;35:1319.
[15] Böker A, Elbs H, Hänsel H, Knoll A, Ludwigs S, Zettl H, et al. Phys Rev Lett 2002;89:135502.
[16] Böker A, Elbs H, Hänsel H, Knoll A, Ludwigs S, Zettl H, et al. Macromolecules 2003;36:8078.
[17] Böker A, Müller AHE, Krausch G. Macromolecules 2001;34:7477.
[18] Anastasiadis SH, Russell TP, Satija SK, Majkrzak CF. Phys Rev Lett 1989;62:1852.
[19] Kozak A, Simon GP, Moscicki JK, Williams G. Mol Cryst Liq Cryst 1990;193:155.
[20] Tsori Y, Andelman D. Macromolecules 2002;35:5161.
[21] Zvelindovsky AV, Sevink GJA. Phys Rev Lett 2003;90:049601.
[22] Böker A, Abetz V, Krausch G. Phys Rev Lett 2003;90:049602.
[23] Schäffer E, Thurn-Albrecht T, Russell TP, Steiner U. Nature 2000;403: 874.
[24] Lin Z, Kerle T, Baker SM, Hoagland DA, Schäffer E, Steiner U, et al. J Chem Phys 2001;14:2377.